www.czasopisma.pan.pl PAN POLSKA AKADEMIA NAUK www.journals.pan.pl

Arch. Metall. Mater. **63** (2018), 4, 1649-1655

DOI: 10.24425/amm.2018.125089

T. SATISH KUMAR*#, K. KRISHNA KUMAR*, S. SHALINI**, R. SUBRAMANIAN*

SYNTHESIS AND CHARACTERIZATION OF FUNCTIONALLY GRADED Al-6Cr-Y_2O_3 COMPOSITES

The present investigation aims at fabricating a functionally graded Al-6Cr-Y_2O_3 composite and its microstructural and property characterization. Al-6Cr-alloys with varying percentage of Y_2O_3 (5-10 vol. %) have been used to fabricate FGM by powder metallurgy route. The samples were subsequently subjected to solution treatment at 610°C for 4 h followed by artificially aged at 310°C for 4 h. The microstructure, hardness and wear behavior of these FGM have been evaluated. FGM exhibited superior hardness (360 ± 5 VHN) as compared to the unprocessed composites (220 ± 5 VHN) due to the uniform dispersion of Y_2O_3 particles. Wear resistance of Al-6Cr-10 Y_2O_3 FGM were compared that of with pure Al-6Cr alloy by dry abrasive wear test. Al-6Cr-10 Y_2O_3 FGM composites were found to exhibit higher wear resistance with the minimum wear rate of 0.009 mm^3/m compared to the Al-6Cr alloy wear rate 0.02 mm^3/m.

Keywords: Al-6Cr alloy, Powder Metallurgy, Functionally graded materials, wear resistance

1. Introduction

Aluminum matrix composites (AMCs) are found to be potential materials with a excellent combination of properties like physical, mechanical, tribological and enhanced elevated temperature properties [1,2]. In particular, Particle-reinforced metal matrix composite materials have received significant importance due to their high strength, high stiffness, higher wear resistance, retention of strength at elevated temperatures and isotropic properties [2-4]. These composites are finding increase in number of applications in aerospace and automobile industries. In a more recent development, Functionally Graded Material composites are receiving increased interest due to their novel property combination.

Functionally Graded Material (FGM) is a new class of advanced engineering materials which exhibit gradual variations in the composition and microstructure with in a component. This leads to achievement of functional performance with unique advantage of the smooth transition in thermal stresses across the cross section and minimum stress concentration at the interface between dissimilar materials. Those FGM are rapidly finding applications in aggressive environments, particularly with steep temperature gradients. Major advantages of FGM are enhanced and location specific functional performance within a component obtained through controlled microstructure [5-8]. FGM can be produced by Physical Vapour Deposition (PVD), Chemical Vapour Deposition (CVD), sol-gel technique, plasma spraying, and Self-propagating High Temperature Synthesis (SHS). Centrifugal casting, molten metal infiltration and powder metallurgy methods can also be used to produce FGM [9-13]. Powder metallurgical processing is one of the most practicable routes for FGM, since composition and microstructure as well as shape forming of FGM can be closely controlled in a wide range [12,14]. Yttrium oxide (Y_2O_3) is a thermodynamically most stable oxide and is appropriate for extreme operation conditions. Yttria a ceramic exhibits typical characteristics of ceramics that are not found in metallic or organic materials, including high hardness (Next to Diamond), high mechanical strength, high temperature stability, erosion resistance [15] as well as chemical resistance [16].

The present study aims at fabrication and characterization of Y_2O_3 reinforced functionally graded composite by the powder metallurgy method. Al-6Cr alloy with 5-10 Y_2O_3 was chosen as the base materials to fabricate FGM composite having progressively increasing hardness and wear resistance from center to periphery of the samples. The composites were characterized and compared with respect to microstructure, hardness and wear characteristics of Al-6Cr alloy.

2. Experimental Work

2.1. Preparation of Al-6Cr-(5-10 vol.%)Y_2O_3 FGM

Commercial 6061 Al alloy powders (30-40 μm, 99%) purity, Cr powders (20-30 μm, 99%) purity, and Y_2O_3 (10-20 μm, 99.8%) purity were used as starting materials. Al, Cr and Y_2O_3

* PSG COLLEGE OF TECHNOLOGY, DEPARTMENT OF METALLURGICAL ENGINEERING, COIMBATORE-641004, TAMILNADU, INDIA
** PSG COLLEGE OF TECHNOLOGY, DEPARTMENT OF PHYSICS, COIMBATORE-641 004, TAMILNADU, INDIA
# Corresponding author: satishmetly@gmail.com

powders were firstly ball milled for 4 h in a stainless steel chamber with a ball to powder ratio of 10:1 at a speed of 650 rpm. The milled powders were then used to prepare the following FGM Al-6Cr, Al-6Cr-5 Y_2O_3 and Al-6Cr-10 Y_2O_3 powder samples. Ball-milled powders were then cold-pressed in a steel mold under the pressure of 200 MPa, sintered at 670°C for 3 h in hot press under an applied pressure of 10 MPa. Sintered samples were subsequently subjected to solution treatment at 650°C for 4 h followed by aging at 310°C for 4 h. The specimens were subjected to microstructural and property investigations.

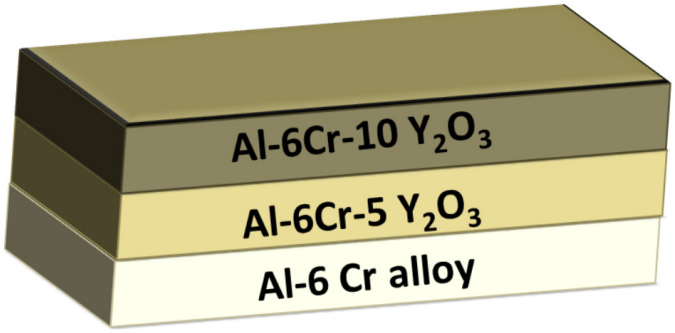

Fig. 1. Section showing different layer in FGM

2.2. Microstructural characterization of the sintered alloy

`X-ray diffraction (XRD-6000, Shimadzu) using Cu Kα (λ =1 .54 Aº) radiation was performed to determine the phases in Al-6Cr/Y_2O_3 FGM. The samples were cut, ground and polished prior to etching using Keller's Reagent solution. The microstructural analysis was carried out using a Carl Zeiss Axio Scope A1 polarized light microscope. Microstructures as well as investigations on worn surfaces of the specimens were characterized using Scanning Electron Microscope (SEM) (JEOL, JSM-6510LV).

To study the effect age hardening on Al-6Cr/Y_2O_3 FGM HRTEM analysis was performed in a JEOL-JEM 2100 microscope, operating at 200 kV. Sample for analysis was prepared by mechanical polishing, followed by electrolytic thinning with a perchloric acid and ethanol solution at room temperature. In the diffraction mode, a pattern of Selected Area Diffraction (SAD) can be recorded by a camera. The diffraction pattern represents a reciprocal lattice plane with reciprocal lattice points shown as the diffraction spots.

The densities of the composites were measured by Archimedes method using water immersion method. Hardness was evaluated using Zwick micro hardness tester under a load of 100 g for 15s and the average value of five measurements was taken as the hardness of the sample.

Dry sliding wear behaviour of the alloy and the synthesized hybrid composites were carried out at room temperature using a pin-on-disc wear and friction monitor (Model TR-20, Ducom, Bangalore). Cylindrical samples of length 30 mm and diameter 10 mm were tested against a hardened EN32 steel disc having hardness of 65 HRC. Pins were ground using different emery papers up to 1200 grit. Pins and counter body surfaces were cleaned using acetone to avoid grease or oil on the surface. Wear rate for the pin was calculated using the Eq. (1) as per ASTM standard G99.

$$W(\mathrm{mm^3 m^{-1}}) = \frac{M(\mathrm{g}) / D(\mathrm{g/mm^{-3}})}{\text{sliding distance (m)}} \tag{1}$$

where: M = mass loss during abrasive wear; D = density of the respective composite

3. Results and discussion

3.1. Morphology and particle size of powders:

The morphology of the as mixed Al-6Cr-10 Y_2O_3 particles showed long rounded irregular particles. It is clear that the particle size and morphology changed with ball milling. During the milling process, the powder particles are subjected to impact when they are caught between the milling media or between the walls of the container and the milling media. When

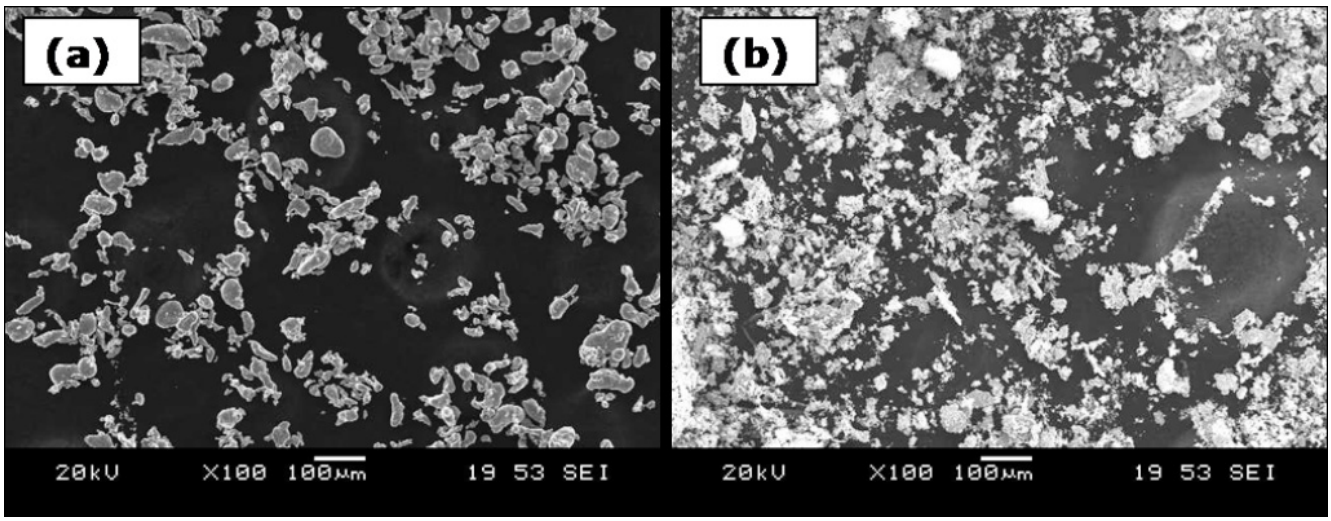

Fig. 2. (a) and (b) shows the SEM images of the Al-6Cr-10 Y_2O_3 powders before and after balling milling for 4h

two or more ductile particles trapped between two colliding balls, they are brought intimate contact and get cold-welded. Cold welding increases the particle size and repeated fracture reduces the particle size [17]. The plastic deformation of the ductile matrix powder occurs rapidly within a short period of milling, resulting in modification of powder particle shape from rounded to flattened large lamellae shaped particles, as reported elsewhere [18-20]. When ductile powders mixed with a brittle material like Y_2O_3 oxide particles, thia leads to an increase in the rate of fracture of milled powders. With continued milling, the lamellae become finer. The already work-hardened particles become more brittle, and their fracture leads to a reduction in particle size.

3.2. Phases and microstructure

The Polarized light micrograph of Al-6Cr-10 Y2O3 FGM (Fig. 3a) shows uniform distribution of Y_2O_3 in Al-6Cr alloy matrix. Y_2O_3 decreases as a function of distance from the periphery of the specimen to 5 vol% Y_2O_3 as shown in Fig. 3b. 5 vol% Y_2O_3 reinforced region also shows uniform distribution of Y_2O_3 in alloy matrix. The microstructure of Al-6Cr alloy region shows cellular α phase with recrystallised grains and small amount of insolubles of Cr with limited amount of porosity.

SEM micrographs show the distribution and morphology of the reinforced Y_2O_3 particles for composites containing varying vol% Y_2O_3. The particles are well distributed homogeneously in the Al-6Cr alloy matrix represented in (Fig. 4). The interface between Al-6Cr matrix and the Y_2O_3 particles appears to be clean and is free from voids.

Fig. 5 shows the consolidated results of X ray diffraction analysis of Al-6Cr-10Y_2O_3 premixed alloy powders and age hardened FGM Composites. After age hardening the Al peaks is displace to lower angle, which indicates the formation of solid solution of Cr in Al. Similar results were reported in case of rapidly solidified Al-Cr alloys by Guofa et al [21]. XRD results further confirmed the presence of Y_2O_3 reinforcement particles and Al_7Cr intermetallic compound formed around partially dissolved Cr particles in the age hardened condition.

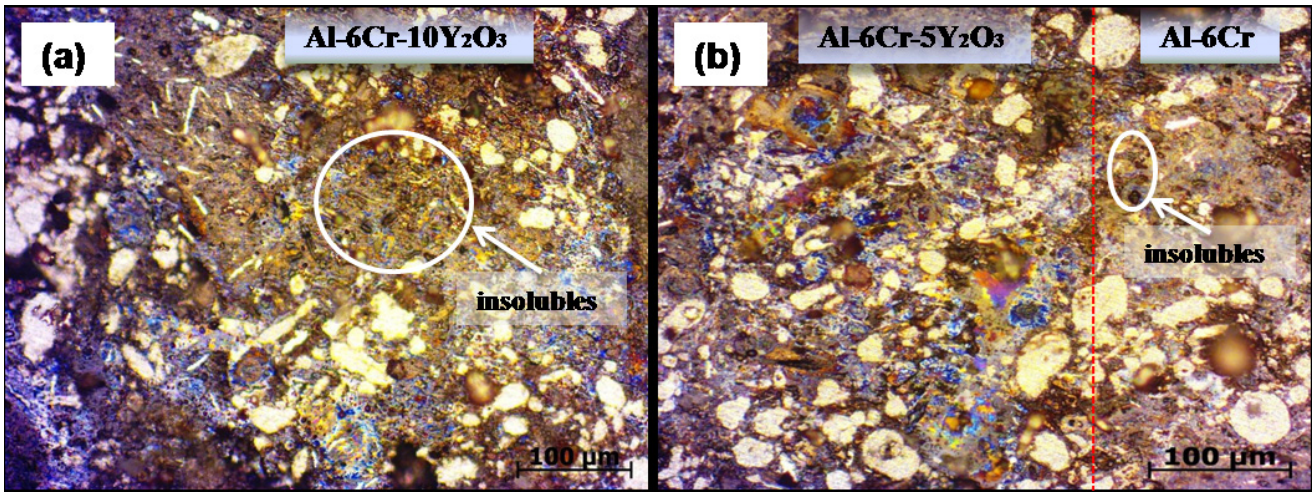

Fig. 3. Polarized light micrograph shows different regions of FGM Al-6Cr alloy a) Al-6Cr-10 Y_2O_3, b) Al-6Cr-5 Y_2O_3 and Al-6 vol% Cr alloy in age hardened condition

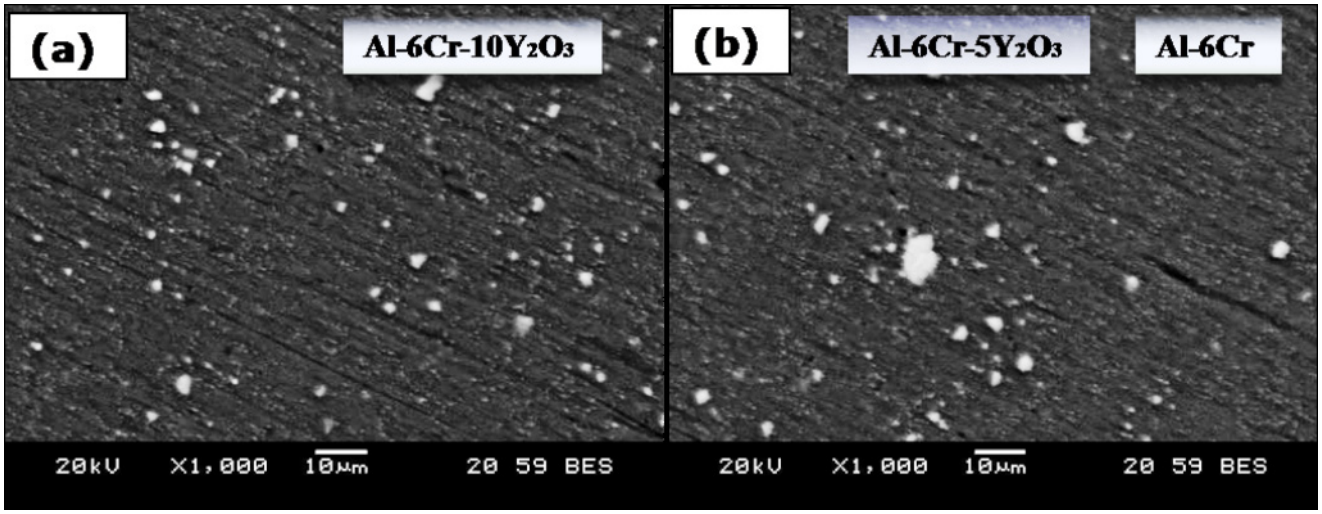

Fig. 4. SEM micrograph shows different regions of FGM Al-6Cr alloy a) Al-6Cr-10 Y_2O_3, b) Al-6Cr-5 Y_2O_3 and Al-6 vol% Cr alloy

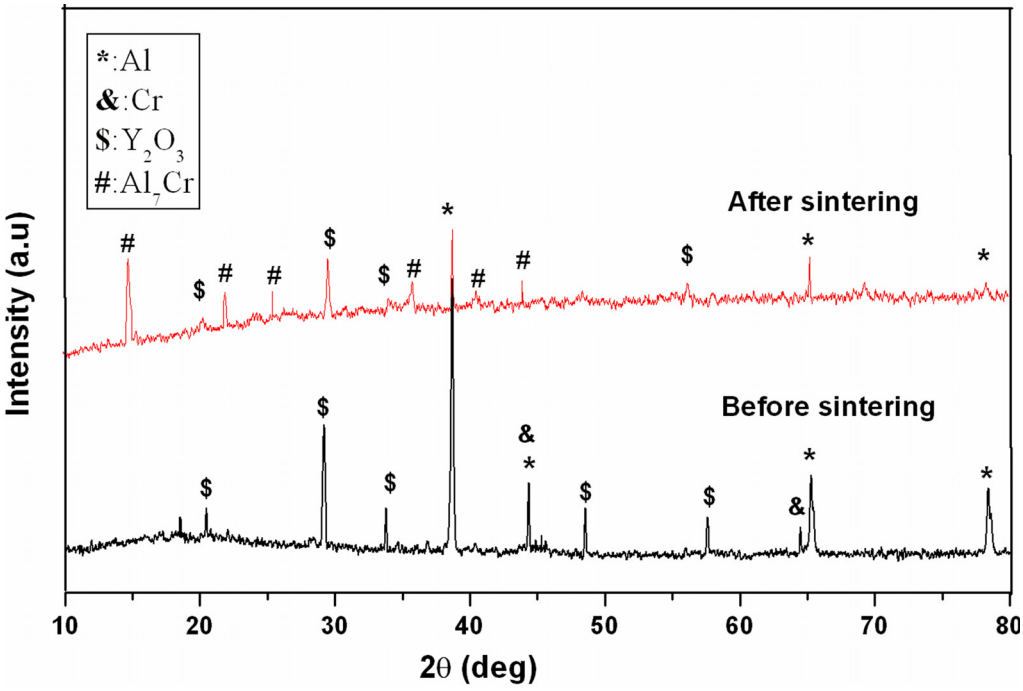

Fig. 5. X-ray diffraction patterns for all the composites

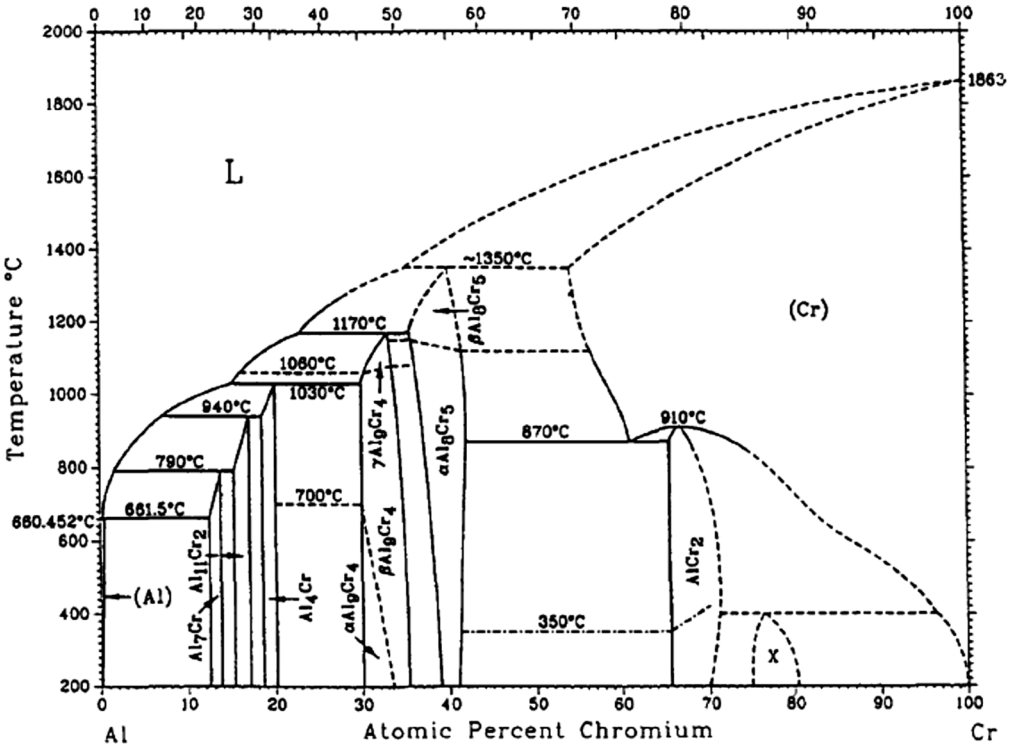

Fig. 6. Al-Cr phase diagram (from Okamoto [22])

Phase diagram of Al-Cr (Fig. 6) shows Al_7Cr phase dissolve at 790°C and a single phase Al solid solution exist in the temperature range of 650-790°C. Hence, two major requirements for a heat-treatable alloy, the existence of a single phase region and the precipitation of intermetallic compounds, are met by the Al-6Cr alloy.

TEM analysis of age hardened Al-6Cr-10 Y_2O_3 FGM Composites.

Detailed microstructural investigation using TEM was done to confirm alloying as well as various phases present. Samples were investigated using with imaging and SAD modes. The diffraction data suggest that the precipitates are consistent with the Al_7Cr phase with monoclinic crystal structure, as reported elsewhere [23]. Fig. 7. Shows the presence of equiaxed particles and the corresponding selected area diffaraction pattern of monoclinic Al_7Cr cell defined by Cooper [24]. This precipitate is

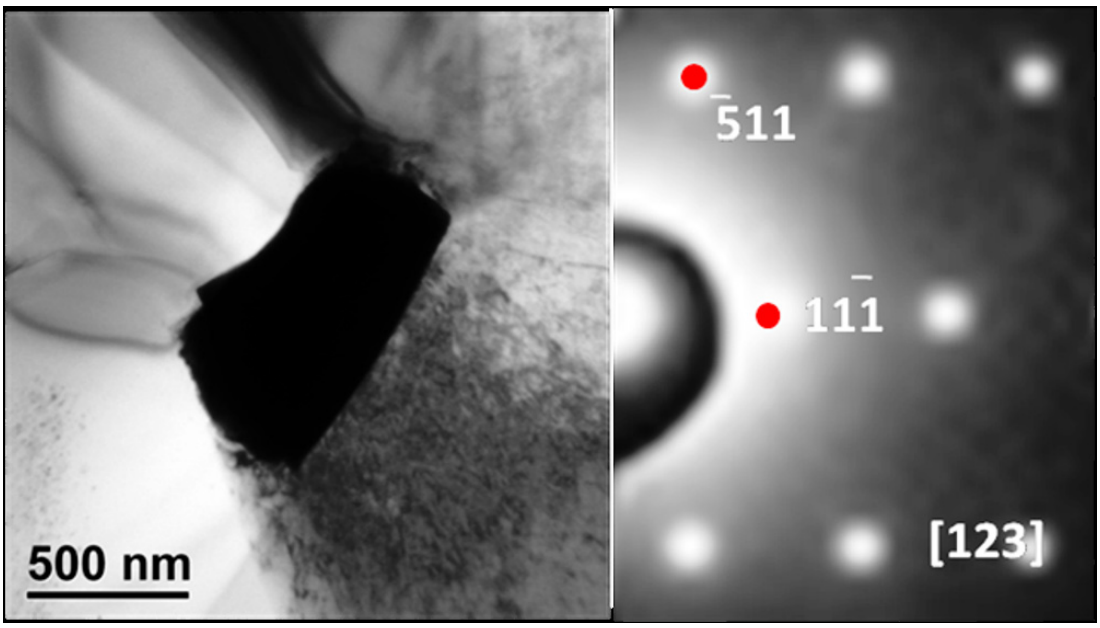

Fig. 7. TEM images of Al_7Cr precipitate and selected area diffraction (SAD) pattern of Al_7Cr precipitate

formed by aluminium and chromium elements from super saturated solution during aging treatment as shown in Al-Cr phase diagram refer (Fig. 6). XRD results further confirmed to TEM analysis. Presence of equiaxed cells comprised of extremely fine Al_7Cr particles (grain size of range 200 nm to 500 nm) and Y_2O_3 particles dispersed in a matrix of α-Al matrix could significantly improve the hardness and wear resistance of FGM Al-6Cr alloy composites. SAD pattern further confirm that sintering results in the formation of strain free grains.

3.3. Evaluation of density of FGM

Very small amount of porosity was observed from the microstructure as seen in Fig. 3. This was further conformed by density measurements by comparing theoretical and actual densities (Fig. 8). Density measurement confirms that the porosity content increased from about 3 to 6% with increase in the Y_2O_3 from 5 to 10 vol. %. Similar results reported by Bishop [25] in case of Titanium / hydroxyapatite functionally gradient material produced by powder metallurgy process. This increase in porosity attributed to the difference in melting points of Al (660°C), Chromium (1,907°C) and Y_2O_3 (2,425°C).

3.4. Hardness measurement

Hardness increases as a function of distance from center (Al-6Cr) to the periphery of (Al-6Cr-10Y_2O_3) as shown in Fig. 9. This is due to presence of more hard Y_2O_3 oxide particles at the external zone compared to the internal zone. Insoluble Cr phase

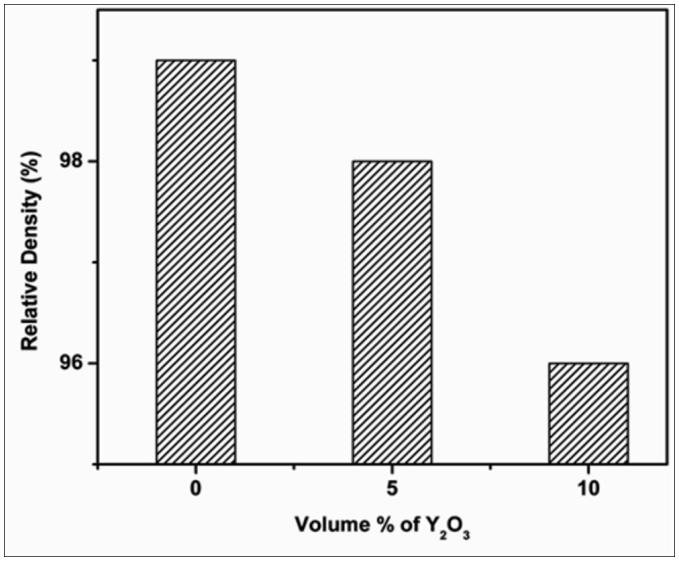

Fig. 8. Variation in density of age hardened Al-6Cr-Y_2O_3 FGM Composites with respect to different vol. % of reinforcement

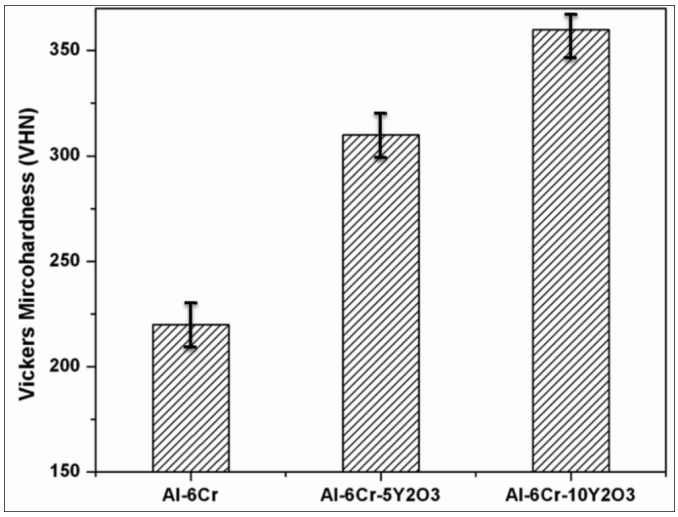

Fig. 9. Variation in Vickers hardness and composition in age hardened FGM

is also likely contributed to increase in hardness of the FGM Al-6Cr alloy. An increase in hardness in excess of 75% is observed center (Al-6Cr) and periphery (Al-6Cr-10Y_2O_3).

3.5. Wear

Wear test results, and wear track analysis were consistent with the microstructural gradient observed in these alloys. In effect, a higher volume density of reinforcing Y_2O_3 in the periphery of the sintered samples exhibits lower wear rate. On the other hand, the internal region with relatively low amounts of Y_2O_3 reinforcement particles and Al-6Cr alloy, exhibited much higher wear rates.

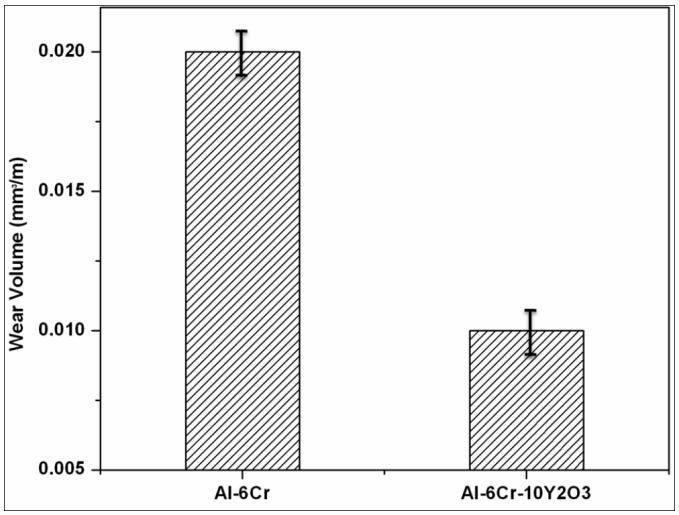

Fig. 10. Wear volume of the age hardened Al-6Cr and Al-6Cr-10 Y_2O_3 samples after undergoing pin-on-disk wear test conducted at 15 N load and a sliding distance of 1000 m

3.5.1. Wear mechanism in FGM

In order to identify the different wear mechanisms that take place in tested wear condition and how the presence of does particles affect them, the worn pins and the wear debris have been analyzed by SEM. The mechanisms observed for the different wear conditions were delamination and abrasion.

3.5.2. Delamination

The predominant wear mechanism is delamination, detachment of the worn surface material in sheet form is produced. This is due to the formation of cracks during the wear process that are perpendicular to the sliding direction and the growth of subsurface cracks that cause the final detachment. Fig. 11a shows the worn surface of Al-6Cr alloy tested at 150 N and sliding distance of 1000 m, as a representative surface morphology of delamination mechanism. The examination of the debris of the samples reveals numerous flakes or sheets (Fig. 11b).

Fatigue produced during sliding induces the subsurface deformation, the crack nucleation and the crack propagation. Hence, the increment of the applied load accelerates this process and delamination wear occurs.

3.5.3. Abrasion

Typical feature of the abrasive wear mechanism is the formation of fine grooves parallel to the sliding direction. Fig. 12a,b shows the worn surface obtained for Al-6Cr-10 Y_2O_3 FGM pin tested at a load of 15 N and a sliding distance of 1000 m and its wear debris n respectively, where the characteristic grooves can be seen indicating that this is the main wear mechanism. These lines are typically caused by hard zones of the counter body surface that plough the soft surface of the Al-6Cr-10 Y_2O_3 pin. This wear mechanism causes the removal of material at the surface forming this kind of paths on the material surface.

Abrasive wear is found to be the predominant wear mechanism in the FGM composites. This behavior can be due to the presence of detached and fractured Y_2O_3 that be get trapped between sliding interface or embedded in the counterface, resulting

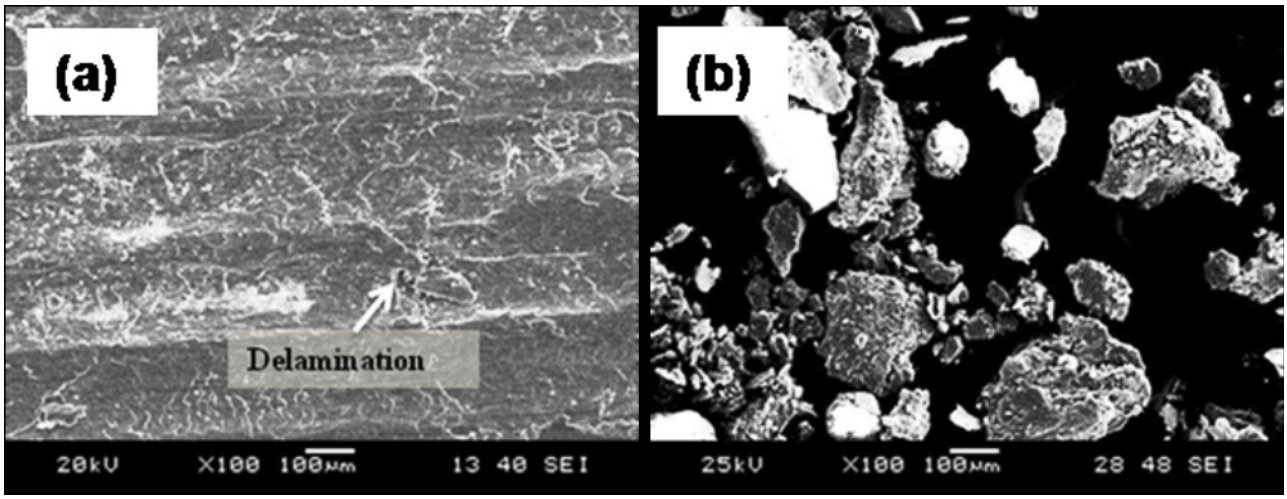

Fig. 11. SEM micrographs of the age hardened (a) Al-6Cr pin surface where voids can be seen; (b) Flakes and sheets in the wear debris

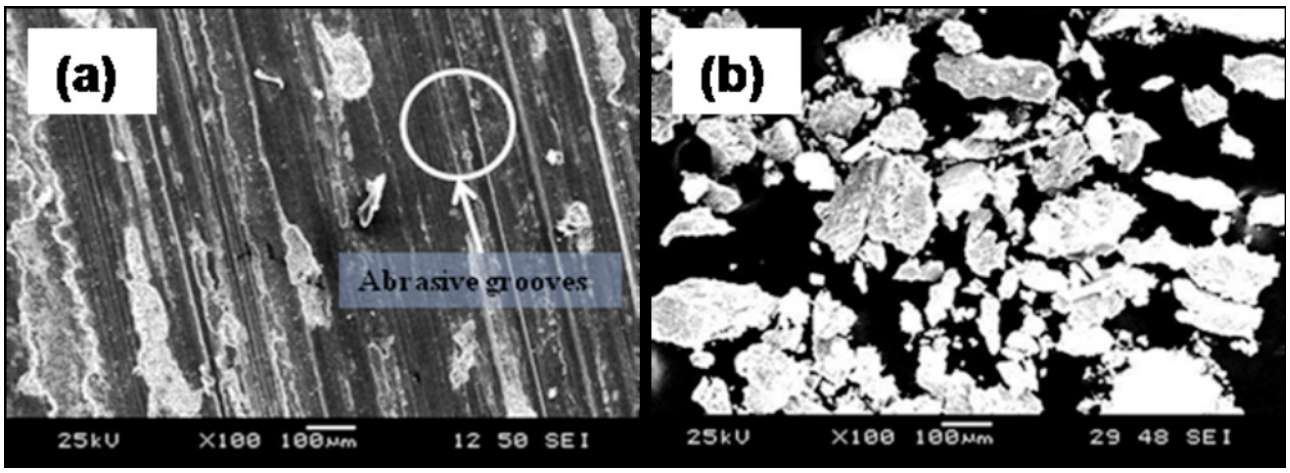

Fig. 12. (a) Grooves and scratch marks on the pin surface of age hardened Al-6Cr-10Y_2O_3 FGM composites tested at 15 N and sliding distance of 1000 m and (b) long elongated shape wear debris

in abrasion of the surface. A similar result has been reported by Lim et al. & García-Rodríguez et al. [12,13] during investigation on wear behavior studies on Al/SiC_p & AZ91/SiCp composites. The debris particles are in the form of long elongated shape (Fig. 12b) and come from the material removed at the surface, confirming the dominant effect of abrasion wear mechanism.

4. Conclusions

The present study aims at fabrication and evaluation of wear behaviour of Y_2O_3 reinforced functionally graded composite produced by powder metallurgy method. Based on the investigation and their results the following conclusions were obtained:

1. Al-6Cr FGM composite from 5 vol.% to 10 vol.% Y_2O_3 was successfully fabricated by powder metallurgy process with premixed powders.
2. The Vickers hardness result showed a variation from 220 VHN to 360 VHN from internal region to periphery region due to the presence of more hard Y_2O_3 particles.
3. Al-6Cr-10 Y_2O_3 FGM composites were found to exhibit higher wear resistance with the minimum wear rate of 0.009 mm^3/m compared to the Al-6Cr alloy wear rate 0.02 mm^3/m.
4. Wear studies on age hardened Al-6Cr alloy exhibited delamination wear, while as Al-6Cr-10 Y_2O_3 FGM composites showed abrasion wear mechanism as the predominant wear mechanism.

REFERENCES

[1] F. Erdemir, A. Canakci, T. Varol, Trans. Nonferrous Met. Soc. China. **25**, 3569-3577 (2015).
[2] T. Satish Kumar, R. Subramanian, S. Shalini, J. Mater. Res. Technol. **4** (3), 333-347 (2015).
[3] T. Varol, A. Canakci, S. Ozsahin, Acta Metall. Sin. Engl. **28**, 182-195 (2015).
[4] A. Canakci, T. Varol, Powder Technol. **268**, 72-79 (2014).
[5] G. Chirita, D. Soares, F.S. Silva, Mater. Des. **28**, 20-27 (2008).
[6] T.P.D. Rajan, B.C. Pai, Acta Metall. Sin. **27**, 825-828 (2014).
[7] J.W. Gao, C.Y. Wang, Mater. Sci. Eng. A **292**, 207-215 (2000).
[8] Z. Yan-boliu, C. Ming, W. Kai, Z. Mao-hua, X. Yong, Trans. Non-ferrous Met. Soc. of China **20**, 361-370 (2010).
[9] S.A. Alidokht, A. Abdollah-zadeh, S. Soleymani, T. Saeid, H. Assadi, Mater. Charact. **63**, 90-97 (2012).
[10] R.S. Rana, R. Purohit, S. Das, Int. J. Sci. Res. Publ. **63**, 90-97 (2012).
[11] J.W. Gao, C.Y. Wan, Mater. Sci. Eng. A **292**, 207-215 (2000).
[12] Z.Y. Ma, A.L. Pilchak, M.C. Juhas, J.C. Williams, Scr. Mater. **58**, 361-366 (2008).
[13] M. Naebe, K. Shirvanimoghaddam, Functionally graded materials: A review of fabrication and properties, Applied Materials Today **5**, 223-245 (2016).
[14] J. Zhu, Z. Lai, Z. Yin, J. Jeon, S. Lee, Mater. Chem. Phys. **68**, 130-135 (2001).
[15] T.C. Joshi, U. Prakash, V.V. Dabhade, DOI: 10.1007/s11665-016-2023-6.
[16] F. Cai, C. Jiang, Zhongquan, Z.V. Ji, Synthesis and characterization of Ni-Al-Y_2O_3 composite coatings with different Y_2O_3 particle content, Ceramics International **40** (9), Part B, 15105-15111 (2014).
[17] B. Prabhu, C. Suryanarayana, L. An, R. Vaidyanathan, Mater. Sci. Eng. A **425**, 192-200 (2006).
[18] T. Varol, A. Canakci, Philos Mag Lett. **93**, 339-345 (2013).
[19] A. Canakci, T. Varol, H. Cuvalci, F. Erdemir, S. Ozkaya, E.D. Yalcın, Micro Nano Lett. **9**, 109-112 (2014).
[20] T. Varol, A. Canakci, S. Ozsahin, Sci. Eng. Compos. Mater. **21**, 411-420 (2014).
[21] M.I. Guofa, M.O. Yalin, W. Kuangfei, Journal of Wuhan University of Technology-Mater. Sci. Ed. **24** (3), 424-427 (2009).
[22] H. Okamoto, Al-Cr (Aluminum-Chromium), J. Phase Equilib. Diff. **29** (1), 112-113 (2008).
[23] M.K. Banerjee, S. Datta, Mater. Charact. **44**, 277-284 (2000).
[24] M.J. Cooper, Acta Crystallogr. **13**, 257(1960).
[25] A. Bishop, C.Y. Lin, M. Navaratnam, R.D. Rawlings, H.B. McShane, J. Mater. Sci. Lett. **12**, 1516-1518 (1993).